Journal of Neurochemistry

JOURNAL OF NEUROCHEMISTRY | 2016 | 136 | 133–147

doi: 10.1111/jnc.13375

ORIGINAL ARTICLE

Microglial Janus kinase/signal transduction and activator of transcription 3 pathway activity directly impacts astrocyte and spinal neuron characteristics

Jenny Molet,*,† Annie Mauborgne,*,† Mickael Diallo,‡ Vincent Armand,*,† David Geny,*,† Luis Villanueva,*,† Yves Boucher*,†,§ and Michel Pohl*,†

*Centre de Psychiatrie et Neurosciences, INSERM UMR 894, Paris, France

†Université Paris Descartes, Paris, France

‡Institute of Physiology, Academy of Sciences, Prague, Czech Republic

§UFR Odontologie, Université Paris-Diderot, Paris, France

Abstract

After peripheral nerve injury microglial reactivity change in the spinal cord is associated with an early activation of Janus kinase (JAK)/STAT3 transduction pathway whose blockade attenuates local inflammation and pain hypersensitivity. However, the consequences of microglial JAK/STAT3-mediated signaling on neighboring cells are unknown. Using an *in vitro* paradigm we assessed the impact of microglial JAK/STAT3 activity on functional characteristics of astrocytes and spinal cord neurons.

Purified rat primary microglia was stimulated with JAK/STAT3 classical activator interleukin-6 in the presence or absence of a selective STAT3 inhibitor and rat primary astrocytes or spinal cord neurons were exposed to microglia conditioned media (CM). JAK/STAT3 activity-generated microglial CM modulated both astrocyte and neuron characteristics. Beyond inducing mRNA expression changes in various targets of interest in astrocytes and neurons, microglia CM activated c-Jun *N*-terminal kinase, STAT3 and NF-κB intracellular pathways in astrocytes and promoted their proliferation. Without modifying neuronal excitability or survival, CM affected the nerve processes morphology and distribution of the post-synaptic density protein 95, a marker of glutamatergic synaptic contacts. These findings show that JAK/STAT3 activity in microglia impacts the functional characteristics of astrocytes and neurons. This suggests its participation in spinal cord tissue plasticity and remodeling occurring after peripheral nerve injury.

Keywords: astrocytes, cell plasticity, JAK/STAT3 pathway, microglia conditioned media, spinal cord neurons.

J. Neurochem. (2016) **136**, 133–147.

Received July 15, 2015; revised manuscript received September 14, 2015; accepted September 15, 2015.

Address correspondence and reprint requests to Michel Pohl, Centre de Psychiatrie et Neurosciences, INSERM UMR 894, Université Paris Descartes, 2ter rue D'Alésia, 75014 Paris, France. E-mail: michel.pohl@inserm.fr

Abbreviations used: ATF3, activating transcription factor 3; BDNF, brain-derived neurotrophic factor; CCL2, chemokine (CC motif) ligand; C-CM, CM from control microglia; CM, conditioned media; COX-2, cyclooxygenase 2; D-CM, CM from microglia incubated with DMSO; G-CSF, granulocyte colony stimulating factor; GFAP, glial fibrillary acidic protein; GLAST, glutamate transporter; GM-CSF, granulocyte macrophage colony stimulating factor; GAPDH, glyceraldehyde-3-phosphate dehydrogenase; HO-1, heme oxygenase-1; I^--CM, CM from microglia incubated with STAT3 inhibitor alone; iNOS, inducible nitric oxide synthase; ITGAM, integrin alpha M; JAK, Janus kinase; JNK MAPK, c-Jun *N*-terminal kinase mitogen-activated protein kinase; KIR4, ATP-sensitive inward rectifying potassium channel; MAP2, microtubule-associated protein 2; NF-κB, nuclear factor kappa B; PSD-95, post-synaptic density protein-95; RS 18S, ribosomal subunit 18S; SOCS3, suppressor of cytokine signaling 3; Stat/I^--CM, CM from microglia incubated with IL-6 in the presence of STAT3 inhibitor; STAT3, signal transduction and activator of transcription 3; STAT-CM, CM from microglia with IL-6-activated STAT3; TLR2 or 4, toll-like receptor 2 or 4; TNFα, tumor necrosis factor-α; xCT, cysteine/glutamate exchanger.

Alteration of glial reactivity in the spinal cord is an important feature of pathological pain (McMahon and Malcangio 2009; Ji *et al.* 2013). Modified glial activity profoundly affects the crosstalk between glial cells and neurons, mobilizing numerous extracellular signaling molecules and intracellular transduction pathways (Suter *et al.* 2007; Grace *et al.* 2014). The activity of Janus kinase (JAK)/signal transducer and activator of transcription 3 (STAT3) pathway plays a major role in neuropoietic cytokine signaling and is linked to the immune/inflammatory reaction (Bauer *et al.* 2007). It was implicated in nerve regeneration, microglia inflammatory response and reactive gliosis following CNS damage (Kim *et al.* 2002; Herrmann *et al.* 2008; Bareyre *et al.* 2011). We previously demonstrated that peripheral nerve injury resulted in an early activation of JAK/STAT3 pathway in rat spinal cord microglia. Under these circumstances, interleukin-6 (IL-6) was a main inducer of microglial JAK/STAT3, the activation of which participated in mechanical allodynia development (Dominguez *et al.* 2008). Local and cell-targeted blockade of this pathway prevented the abnormal expression of several markers induced after peripheral nerve injury and attenuated mechanical pain hypersensitivity in rats (Dominguez *et al.* 2010). Interestingly, the adipokine leptin that signals downstream through JAK/STAT3 also contributes to neuropathic pain induction (Lim *et al.* 2009). Peripheral nerve injury was also found to promote JAK/STAT3 activity in spinal astrocytes, participating in reactive astrogliosis and mechanical allodynia maintenance (Tsuda *et al.* 2011). Collectively, these data suggest the participation of glial JAK/STAT3 signaling in spinal tissue plasticity, a hallmark of neuropathic pain emerging after peripheral nerve injury.

Understanding the specific role of the early activated JAK/STAT3 in spinal microglia in relation to other neighboring cell types seems however difficult *in vivo*. In particular, after peripheral nerve injury and associated inflammatory and glia reactivity changes in the spinal cord, many cell types, including altered primary sensory neurons, release similar signaling molecules that participate in complex cellular crosstalk (Grace *et al.* 2014). In this study, we explored the role of JAK/STAT3 activity in microglial interactions with astrocytes and neurons using an *in vitro* cell culture approach. Microglial JAK/STAT3 pathway was stimulated with the prototypical activator IL-6 and microglial culture media (conditioned media, CM) were generated under different experimental conditions. We then assessed their impact on functional aspects of astrocytes and neurons, focusing on several characteristics of spinal alterations associated with neuropathic pain.

Materials and methods

Animals

Gestating rats and females with littermates (Sprague Dawley rats; Janvier Labs, Saint Berthevin, France) were maintained under controlled conditions (22 ± 1°C, 60 ± 10% relative humidity, 12 h light/dark cycle, food and water *ad libitum*). Experiments were performed in line with institutional guidelines, to comply with national and international laws and policies for the use of animals in neuroscience research (European Communities Council Directive 87848, October 1987, Ministère de l'Agriculture et de la Forêt, Service Vétérinaire de la Santé et de la Protection Animale; Permission B-75-1179 to M.P.; authorization no. 13–033 Comité d'Ethique Université Paris Descartes).

Primary cell cultures

Glial cells were prepared from spinal cords or cerebral cortices of 1- to 3-day-old rat pups following described procedures with slight modifications (Goslin *et al.* 1998; Mecha *et al.* 2011). Spinal cords or cerebral cortices were dissected and meninges (together with attached dorsal root ganglia in spinal cord tissue) were removed. Tissue from 6 to 8 pups were dissociated in Hank's Balanced Salt Solution (HBSS) containing 50 mM HEPES and centrifuged (200 *g*, 30 s). The pellet was suspended in 10 mL HBSS containing 50 mM HEPES, 0.25% trypsin and 0.2 mg/mL DNAse I, and incubated 15 min at 37°C. After adding trypsin inhibitor (0.25 mg/mL), tissue was dissociated with Pasteur pipette trituration. Tissue suspension was centrifuged (200 *g*, 10 min) and pellet was suspended in 50 mL Dulbecco's modified Eagle's medium supplemented with 10% heat-inactivated fetal calf serum and 1% (w/v) penicillin/streptomycin (complete culture medium). The suspension was centrifuged as above until a clear supernatant was obtained. The final pellet was suspended in complete medium and seeded in 75 cm^2 culture flask (Corning Life Sciences via VWR International). Culture medium was replaced 24 h later with fresh complete medium and cells were further incubated 14 days (37°C, water saturated 95% air/5% CO_2 atmosphere) without changing the medium.

Microglial cells were isolated from mixed glia cultures at day 14 by flask shaking (230 rpm orbital shaker, 3 h, 37°C). Resulting culture medium was saved for microglia isolation and flasks were loaded with 37°C warm complete medium for further astrocytes preparation. Saved medium was centrifuged (200 *g*, 10 min) and the pellet was suspended in 1 mL/initial flask of warm complete medium. Microglial cells were counted and seeded at a density of 70 000 cells/cm^2 on poly-D-lysine-coated six-well plates for semi-quantitative RT-PCR experiments and CM generation or in four-well plates at a density of 25 000 cells/cm^2 on poly-D-lysine-coated 12-mm diameter coverslips for immunocytochemistry.

For astrocytes preparation, original flasks were completely closed and further shaken overnight. The medium (mostly containing oligodendrocyte progenitor cells) was discarded and remaining attached cells were washed with phosphate-buffered saline (PBS) then incubated with trypsin/EDTA (0.05%/0.02%; Invitrogen, Carlsbad, CA, USA) solution (5 min; 37°C). Five milliliters of complete medium was added to stop trypsin activity, the medium was centrifuged (200 *g*, 10 min) and resulting pellet suspended in 5 mL/flask of complete medium. Cells were seeded in a 75 cm^2 culture flask, propagated during 1 week and collected again after trypsin/EDTA incubation as above. Astrocytes, used at 20–40 days *in vitro* (DIV), were seeded in six-well plates for western blots, PhosphoTracer assay and semi-quantitative RT-PCR experiments (50 000 cells/cm^2) or in four-well plates containing poly-D-lysine-coated 12-mm diameter coverslips for immunocytochemistry

(25 000 cells/cm^2). For proliferation studies, 24 h after their seeding in four-well plates, culture medium was replaced and astrocytes were further grown for 24 h in serum-free conditions before their incubation with different microglia-derived CM.

Spinal cord neurons were prepared from E17 rat embryos as described previously (Meunier *et al.* 2007). Cells were counted and plated on six-well plates containing three poly-D-lysine-coated 14-mm diameter coverslips per well for semi-quantitative RT-PCR experiments (50 000 cells/cm^2) or in four-well plates containing one poly-D-lysine-coated 12-mm diameter coverslip per well for immunocytochemistry (25 000 cells/cm^2). Four hours after plating, the culture medium was replaced by sterile-filtered conditioned medium obtained by incubating mixed glial cell cultures (~ 70% confluency) for 24 h in the complete medium described above. Neurons were kept in the same medium 4 DIV then incubated with microglia-derived CM and processed for different experiments.

Microglia CM generation and experimental use

JAK/STAT3 pathway was activated in purified microglia by incubating (or not) the cells 6 h with 10 ng/mL of rat recombinant IL-6 (Peprotech, Neuilly-sur-Seine, France). Blockade of STAT3 signaling was achieved with 100 μM of STAT3 inhibitor VI (Merck, Lyon, France) solubilized in dimethylsulfoxide (DMSO) (0.36% final). Cells were pre-incubated 15 min in control, 0.36% DMSO- or STAT3 inhibitor containing medium. Culture media were replaced by new media containing IL-6 or not (control, DMSO control, 100 μM STAT3 inhibitor containing medium, IL-6 in 0.36% DMSO medium, IL-6 in 100 μM STAT3 inhibitor containing medium). After 6 h incubation, cells were thoroughly washed with Dulbecco's PBS (3×; Invitrogen) and then with culture medium (2×) to minimize the presence of residual traces of IL-6, and covered with 1.1 mL of pre-warmed glial culture medium. After further 2 h incubation, culture media were collected, centrifuged (200 *g*, 10 min, 4°C) and 1 mL of final supernatant was stored at −80°C until use. Cells were rinsed in Dulbecco's PBS before total RNA extraction.

Typically, five different experimental conditions generated respective conditioned media: control microglia (C-CM), microglia incubated with DMSO, microglia incubated with STAT3 inhibitor alone (I$^-$-CM), microglia with IL-6-evoked STAT3 activity (Stat-CM) and microglia incubated with IL-6 in the presence of STAT3 inhibitor (Stat/I$^-$-CM). This protocol, adopted after a pilot work, showed that microglia stimulation for 6 h followed by the collection of STAT3 activity-generated secreted molecules during 2 h, produced CM with most reliable effects.

For experiments, CM were thawed on ice, pooled from several preparations, pre-warmed to 37°C and 1 or 0.3 mL of CM was applied on 24 h serum-starved astrocytes in six- or four-well plates, respectively. Astrocytes were incubated 24 h in the presence of CM for cell proliferation study, 6 h for mRNA expression analyses, 1 h or 30 min for different PhosphoTracers ELISA assays and nuclear factor kappa B (NF-κB) nuclear translocation evaluation.

Six- or four-well plates containing spinal neurons were covered with 1 or 0.3 mL of CM respectively. Cells were incubated either 24 h (or 48 h in some experiments) with CM for neuron survival evaluation, patch-clamp experiments, neuronal processes morphology and study of synaptic contacts, or 6 h for mRNA expression analyses.

TaqMan® gene expression assay and real-time RT-PCR analysis

Total RNA was extracted from cell cultures using NucleoSpin® RNA II Purification Kit (Macherey-Nagel, Hoerdt, France) and their quality and concentrations were evaluated by optical density using NanoDrop (Thermo Scientific, Labtech, Villebon sur Yvette, France).

For real-time RT-PCR analysis, first-strand cDNA synthesis (0.6 μg total RNA per 20 μL reaction) was carried out with a High-Capacity cDNA Reverse Transcription Kit (Applied Biosystems, Saint-Aubin, France). TaqMan® 'mouse immune response' gene expression array was used for an initial screening of immune response-related genes expression in astrocytes incubated with different CM. Twenty-five nanograms of cDNA per well in 96-well plates were used and RT-PCR on the ABI Prism 7300 (Applied Biosystems) were then processed following the manufacturer's recommendations.

Real-time PCR amplification for various individual mRNA in each sample was performed in triplicate on the ABI Prism 7300 using ABgene Absolute QPCR ROX Mix (ABgene, Saint-Aubin, France). Assay-on-Demand Gene TaqMan PCR probes (Applied Biosystems) were used for target genes: suppressor of cytokine signaling 3 (SOCS3; Rn00585674_s1), glial fibrillary acidic protein (GFAP, Rn01460868_m1), integrin alpha M (Rn00709342_m1), granulocyte colony stimulating factor (G-CSF; Rn00567344_m1), granulocyte macrophage colony stimulating factor (GM-CSF; Rn01456851_m1), IL-6 (Rn00561420_m1), IL-1β (Rn00580432_m1), IL-18 (Rn99999185-m1), chemokine (CC motif) ligand 2 (CCL2; Rn00580555_m1), tumor necrosis factor-α (TNFα; Rn99999017_m1), brain-derived neurotrophic factor (Rn00560868-m1), activating transcription factor 3 (Rn00563784_m1), inducible nitric oxide synthase (iNOS; Rn00561646_m1), cyclooxygenase-2 (COX-2; Rn01483828_m1), toll-like receptor 2 (TLR2; Rn02133647-s1), toll-like receptor 4 (TLR4; Rn00569848-m1), glyceraldehyde-3-phosphate dehydrogenase (GAPDH; Rn99999916_s1), ribosomal subunit 18S (RS 18S; Hs99999901_s1), heme oxygenase-1 (HO-1; Rn01536933_m1), cystine/glutamate exchanger (xCT; Rn0145123_m1), glutamate transporter (GLAST; Rn00570130_m1), ATP-sensitive inward rectifying potassium channel (KIR4; Rn01639245_m1), connexin 43 (Rn01433957_m1), microtubule-associated protein 2 (MAP2; Rn00565046_m1).

To perform semi-quantitative studies, GAPDH and RS 18S were used as reporter genes. Because the relative expression of GAPDH compared with RS 18S was not significantly different in cells under various experimental conditions, most of the experiments were performed with GAPDH as reporter gene.

PhosphoTracer ELISA

The activity of c-Jun *N*-terminal kinase mitogen-activated protein kinase (JNK MAPK), STAT3 and NF-κB pathways was assessed in astrocytes using PhosphoTracer ELISA kits (Abcam, Paris France). Astrocytes were incubated or not with different CM during 30 min for JNK 1/2/3 (# ab119625; Thr 183, Tyr 185) and STAT3 (# ab119650; Tyr 705) or 1 h for NF-κB p65 (# ab119636; Ser 536) phosphorylation assay. Cells were washed with PBS, covered with 250 μL of cell lysis solution and lysates (50 μL/well, each experimental condition in triplicate) were transferred in specific PhosphoTracer microplates then processed following manufacturer's recommendations. Fluorescence signals were determined using En Vision 2101 Multireader (PerkinElmer, Villebon sur

Yvette, France) and data expressed in raw fluorescence units (RFU) were pooled from three distinct experiments for comparison.

Immunocytochemistry

The primary antibodies used for this study were mouse anti-GFAP (1 : 5000; Chemicon International, Billerica, MA, USA), rabbit anti-Iba1 (1 : 800; Wako Chemical, Richmond, Virginie, USA), mouse anti-MAP2 (1 : 500; Cell Signaling Technology, Beverly, MA, USA), mouse anti-post-synaptic density protein-95 (PSD-95; Sigma, Evry, France), mouse anti-KI-67 (1 : 200; Cell Signaling Technology) and rabbit anti-NF-κB p65 (1 : 100; Santa Cruz Biotechnology, Heidelberg, Germany). Secondary antibodies used were Alexa 488- or 594-conjugated donkey anti-rabbit and anti-mouse Ig (1 : 500; Invitrogen).

Cells were prepared for fluorescent immunochemistry as described previously (Meunier *et al.* 2007). Briefly, after fixation in 4% paraformaldehyde in PBS, coverslips with cells were washed with PBS containing 0.1 mM $CaCl_2$ and 0.1 mM $MgCl_2$ (PBS+) and incubated with blocking buffer (3% donkey serum and 0.3% Triton X-100 in PBS+). Cells were then incubated in the same buffer with primary antibody (2 h, RT, 21–22 °C), washed with PBS+ and incubated with secondary antibodies in blocking buffer (1 h, RT, 21–22 °C). Coverslips were rinsed (PBS+) and mounted in Fluoromount-G solution (Clinisciences, Nanterre, France).

Slides were observed with a fluorescent microscope (Axio Imager M1; Carl Zeiss, Fougères, France) and images were obtained with a digital camera (Axio Cam HRC; Carl Zeiss) equipped with image-acquisition software (Axio Vision; Carl Zeiss).

Western blotting

Cell cultures were washed three times in ice-cold PBS and were scraped in 1 mL of this solution. Samples were centrifuged (1.500 *g*, 3 min, 4°C) and pellets were suspended in Radio-immunoprecipitation Assay Buffer (20 mM Tris pH = 7.5, 150 mM NaCl, 1% NP40, 0.5% Na deoxycholate, 1 mM EDTA, 0.1% sodium dodecyl sulfate) supplemented with a protease and phosphatase inhibitor cocktail (Sigma-Aldrich, Evry, France). Samples were stored at −80°C until use. Western blots were processed as described previously (Dominguez *et al.* 2010) using rabbit anti-pSTAT3 (tyr 705; 1 : 500; Cell Signaling Technology) antibody, mouse anti-α-tubulin (1 : 10 000; Amersham Biosciences, Piscataway, New Jersey, USA) or, in some experiments, rabbit anti-STAT3 (1 : 750; Cell Signaling Technology) antibody. Blotted (Trans-Blot Turbo™; Bio-Rad Laboratories, Colmar, France) polyvinylidene difluoride membranes were scanned on an Odyssey Infrared Imaging System (Li-cor Biosciences, Lincoln, Nebraska, USA) and the density of the pSTAT3 and STAT3 immunoreactivity were compared to α-tubulin controls using Odyssey Image Studio analysis software (Hach, Düsseldorf, Germany).

Astrocytes proliferation and neurons morphological changes

The KI-67 protein detection in cell nuclei was used to evaluate astrocytes proliferation. After 24 h incubation with CM, cells presenting nuclear labeling for KI-67-like immunoreactive material (IR) (both mild and strong KI-67 labeling) and Hoechst-labeled cell nuclei were counted in three randomly selected microscope fields for each condition in 5–6 different experiments. Data were expressed as the number of KI-67 labeled cell nuclei on the total number of astrocyte nuclei (Hoechst stained).

The impact of CM on primary neuron survival was evaluated by comparing the number of NeuN-stained cells following 24 h (or 48 h in some experiments) exposure to different CM. Similarly, morphological and connectivity characteristics of spinal neurons were evaluated using MAP2- and PSD-95-labeling density measurement. In three distinct experiments and for each CM condition, five microscope fields were randomly selected. For MAP2 and PSD-95 labeling density comparison, images, acquired using a confocal microscope (Leica TCS SP5, Nanterre, France) with a 40× oil objective and a PhotoMultiplierTube as detector, were treated using Volocity software (PerkinElmer) for deconvolution and measurement of PSD-95/MAP-2-stained volume ratio under different experimental conditions. The length of neuronal processes was measured using Image J software (National Institutes of Health, Bethesda, MD, USA) in randomly selected neurons (five neurons in each CM culture condition from three distinct experiments were evaluated).

Electrophysiological recordings of primary spinal neurons

Two days after neuron incubation in the presence of different CM, coverslips with attached neurons (25 000 cells/cm^2) were transferred into a bath solution consisting of 144 mM NaCl, 3.5 mM KCl, 2.5 mM $CaCl_2$, 1.5 mM $MgSO_4$, 1.2 mM NaH_2PO_4, 10 mM HEPES, $NaHCO_3$, 10 mM Glucose, pH 7.3, 310–320 mOsm/L. Cells were visualized using Olympus IX 50 microscope. The patch pipettes were pulled from thin-walled borosilicate glass capillaries (1.5 mm outer diameter) with a BBCH horizontal pipette puller (Mecanex, Nyon, Switzerland). The initial input resistance of the recording pipettes was 3.5–6 MΩ when filled with intracellular solution. Pipettes were filled with 130 mM K-Methane sulfonate, 1.1 mM EGTA, 2 mM $MgCl_2$, 10 mM HEPES, 2 mM Na_2 ATP, 3 mM KCl, pH 7.3 (adjusted with 1 M KOH), 290–300 mOsm/L. After obtaining a high-resistance GΩ seal and achievement of whole-cell access, recordings were performed at room temperature (21–22°C) through at least 15 min for each neuron using an Axopatch 1D amplifier (Axon Instruments, Union City, CA, USA), digitized using a Digidata 1200 interface (Axon Instruments) and stored on a computer.

Statistical analysis

Data are presented as means ± SEM. For RT-PCR data, the $2^{-\Delta\Delta Ct}$ method (Livak and Schmittgen 2001) was used to analyze the relative differences in specific mRNA levels between groups (RQ Study Software 1.2 version; Applied Biosystems). Data generated from TaqMan® gene expression assay were analyzed using DataAssist™ Software v0.50 (Life Technologies). Data for RT-PCR, PhosphoTracer ELISA approaches, electrophysiological recordings and immunocytochemistry examination of astrocytes proliferation and neurons morphology were processed by one-way ANOVA with Bonferroni *post hoc* test. Statistical evaluation was performed with PRISM4 software (GraphPad, San Diego, CA, USA). In all statistical comparisons, $p < 0.05$ was considered significant.

Results

Conditioned media generation from purified primary microglia cell cultures

Microglia cultures typically contained > 97% of Iba-1-labeled microglial cells and < 3% of GFAP-labeled

astrocytes (not shown). Incubation of microglia with recombinant rat IL-6 (10 ng/mL, 30 min) led to rapid accumulation of the phosphorylated (active) form of STAT3 (pSTAT3) (Fig. 1a). IL-6-evoked pSTAT3 accumulation was abolished in the presence of specific STAT3 inhibitor (100 μM STAT3 inhibitor VI; Merck); STAT3 inhibitor alone had no effect on pSTAT3 levels. We further evaluated the IL-6 effect and the STAT3 inhibitor VI (STAT3 I$^-$) efficacy on SOCS3 mRNA expression that is mediated through JAK/STAT3 pathway activity (Dominguez *et al.* 2010). As expected, stimulation of microglia with IL-6 (10 ng/mL, 6 h) evoked SOCS3 mRNA up-regulation ($\times 8.40 \pm 0.51$) that was significantly attenuated in the presence of STAT3 inhibitor (100 μM, $p < 0.001$) (Fig. 1b). Incubation of cells in the presence of STAT3 I$^-$ alone did not affect the levels of SOCS3 mRNA.

In microglia, we first evaluated the impact of JAK/STAT3 activation on the expression of classical immune response-related genes. Expression changes evoked through JAK/STAT3 pathway were screened using TaqMan® 'immune response' gene expression array (not shown). Data obtained from this approach were confirmed and extended to other potential targets, known for their role in pain pathophysiology, using semi-quantitative real-time RT-PCR. A complete list of analyzed targets is provided in Table S1. As shown in Fig. 2, in addition to SOCS3 mRNA, 6 h microglia stimulation with IL-6 induced expression of mRNAs encoding molecules such as cytokines (IL-6, IL-18, TNFα, G-CSF, GM-CSF), chemokines (CCL2), trophic factors (brain-derived neurotrophic factor) and enzymes (iNOS). With the exception of up-regulated TNFα mRNA, the IL-6-evoked increased

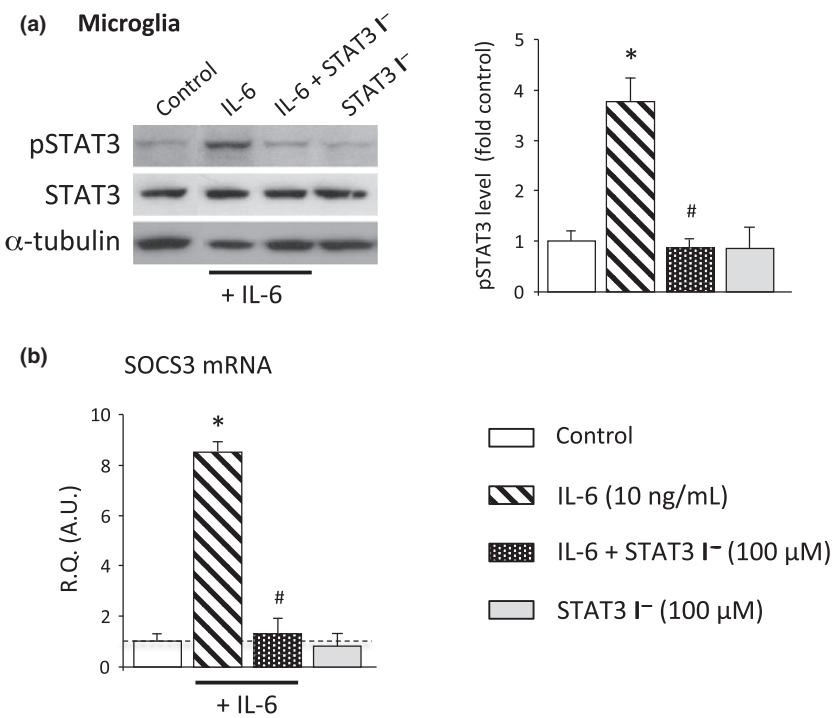

Fig. 1 IL-6-evoked Janus kinase/signal transduction and activator of transcription 3 (STAT3) activity in primary microglia is effectively blocked by STAT3 inhibitor. (a) Western blot analysis of protein extracts from rat primary microglia control culture showed low basal levels of the phosphorylated form of STAT3 protein (pSTAT3). Incubation of cells with IL-6 (10 ng/mL, 30 min) resulted in pSTAT3 accumulation that was prevented in the presence of specific STAT3 inhibitor (100 μM, STAT3 inhibitor VI; Merck). Incubation of cells with STAT3 inhibitor alone did not affect the pSTAT3 levels. The levels of STAT3 protein remained comparable in different experimental conditions. Relative intensities of the pSTAT3 and STAT3 immunoreactivity were compared with α-tubulin controls using scanned images of the blots. Data represent the mean ± SEM of three different experiments ($n = 3$). (b) Concentration of suppressor of cytokine signaling 3 (SOCS3) mRNA, deriving from a classical STAT3 transcription factor target gene, *SOSC3*, was enhanced in microglia incubated with IL-6 (10 ng/mL, 6 h). SOCS3 mRNA level increase was almost completely blocked in the presence of STAT3 inhibitor. Real-time RT-PCR relative quantification (R.Q.) in arbitrary units (A.U.) corresponds to the ratio of specific mRNA over glyceraldehyde-3-phosphate dehydrogenase mRNA. The dotted line represents the relative quantification of SOCS3 mRNA determined in control microglia cultures. Each bar is the mean ± SEM ($n = 5$ for each experimental condition). $^*p < 0.05$, IL-6 treated cells versus control cells; $^\#p < 0.05$, cells treated with IL-6 in the presence of STAT3 inhibitor versus IL-6 treated cells.

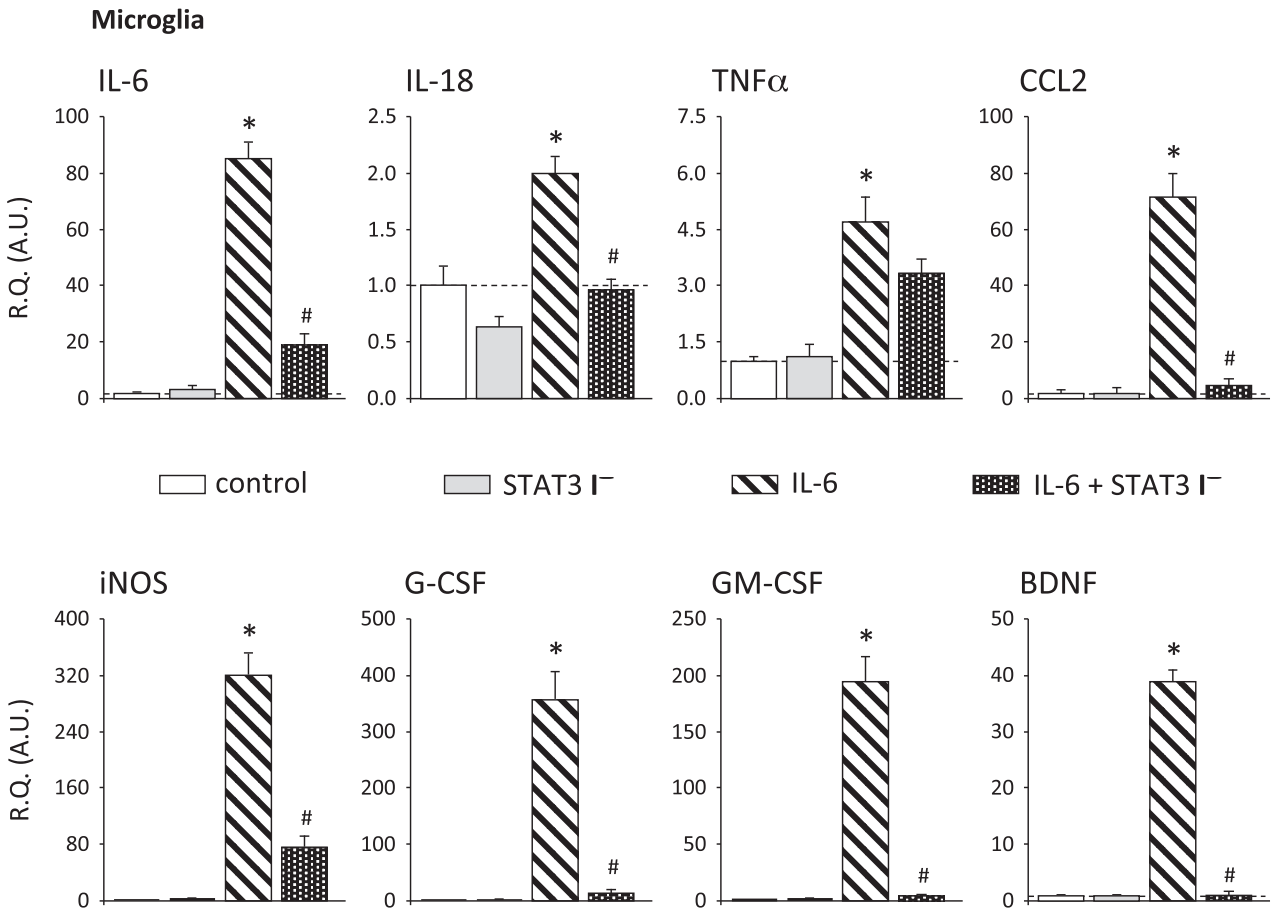

Fig. 2 Blockade of microglial Janus kinase/signal transduction and activator of transcription 3 (STAT3) activity inhibits the IL-6-evoked expression of mRNAs encoding various proteins with known implication in neuropathic pain. Primary microglia was stimulated with IL-6 (10 ng/mL, 6 h) in the presence or absence of STAT3 inhibitor (100 μM). Excepting TNFα mRNA, the IL-6-evoked up-regulation of other explored markers [IL-6, IL-18, CCL2, granulocyte colony stimulating factor (G-CSF), granulocyte macrophage colony stimulating factor (GM-CSF), brain-derived neurotrophic factor (BDNF), iNOS] was efficiently prevented by STAT3 blockade. Each bar is the mean ± SEM (n = 5–6 for each experimental group). *$p < 0.05$, IL-6 treated cells versus control cells; #$p < 0.05$, cells treated with IL-6 in the presence of STAT3 inhibitor versus IL-6 treated cells. R.Q., relative quantification; A.U. arbitrary units.

expression of all other assessed markers was prevented in the presence of STAT3 I⁻.

Effect of microglial CM on the characteristics of astrocytes

Signal transduction pathways

To assess the consequences of JAK/STAT3 activation in microglia on astrocyte functional characteristics, overnight serum-starved astrocytes were incubated with different CM. We first analyzed the impact of CM on intracellular pathways activation, focusing in particular on JNK MAPK, STAT3 and NF-κB systems whose roles in the modulation of astrocyte reactivity state have been reported (Gao *et al.* 2009; Tsuda *et al.* 2011; Yin *et al.* 2015). The PhosphoTracer ELISA assay revealed the presence of phosphorylated forms of these proteins and showed that, compared with control CM (C-CM), incubation of astrocytes with CM from IL-6-stimulated microglia (Stat-CM) led to the significant accumulation of phosphorylated forms of JNK, STAT3 and p65 subunit of NF-κB (Fig. 3a). By contrast, Stat/I⁻-CM evoked no accumulation of phosphorylated forms of JNK or STAT3. For P-p65 NF-κB in astrocytes treated with Stat/I⁻-CM, the fluorescence was higher than in the presence of C-CM (Fig. 3a), albeit non-significantly. We further explored the modulation of astrocyte NF-κB pathway activity by CM through the assessment of the p65 NF-κB subcellular distribution in immunocytofluorescence experiments. In astrocytes incubated with C-CM, p65 NF-κB-IR was homogenously distributed throughout the cell cytoplasm (Fig. 3b). Treatment of astrocytes with Stat-CM resulted in rapid p65 NF-κB-IR translocation and accumulation in cell nuclei. This activating effect was absent in cells incubated with Stat/I⁻-CM in which p65 NF-κB-IR remained mainly localized in the cytoplasm.

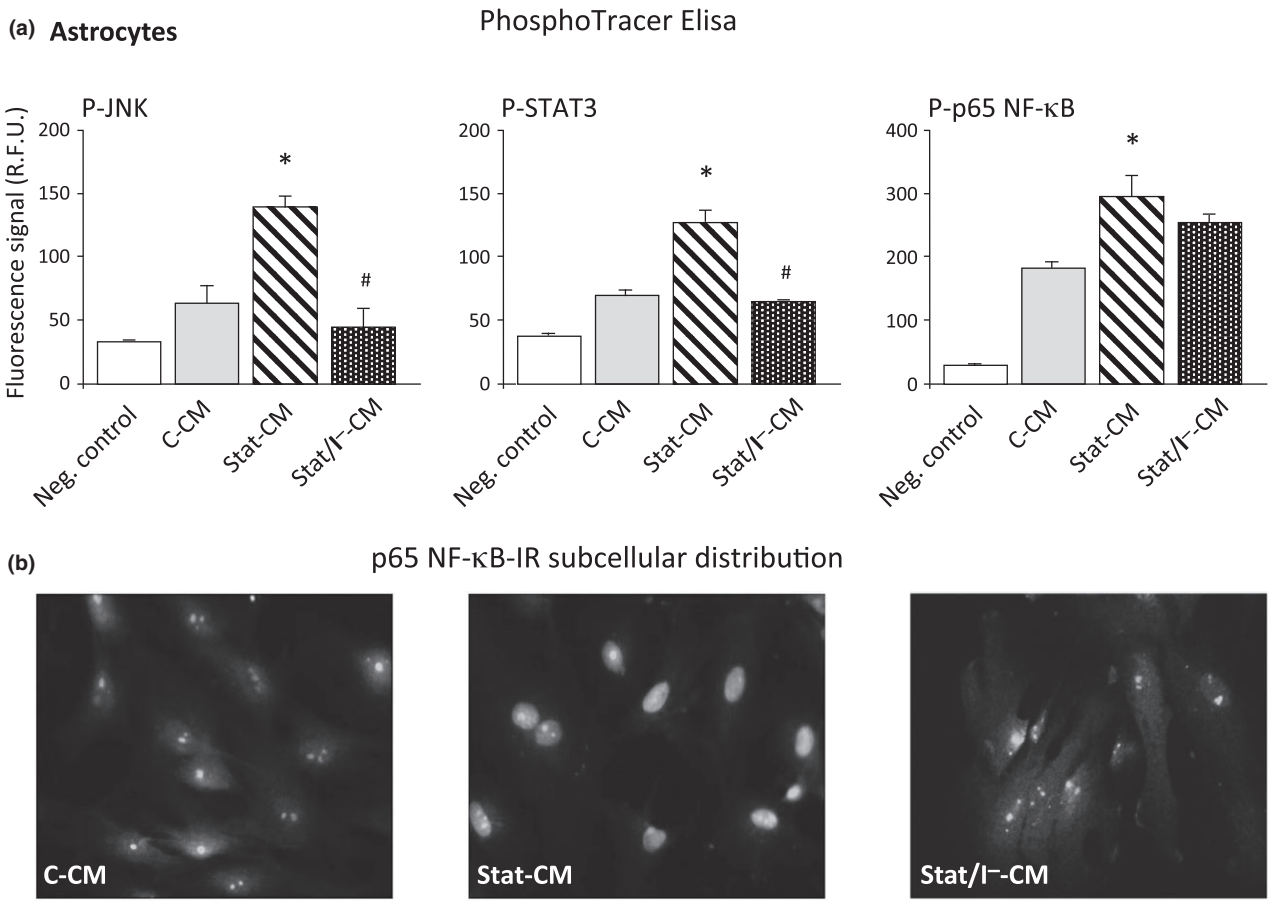

Fig. 3 Microglial Janus kinase/signal transduction and activator of transcription 3 (STAT3) activity-generated conditioned media modulated several intracellular transduction pathways in astrocytes. Pure rat primary astrocytes were incubated for 30 min (JNK and STAT3 activity) or 1 h (NF-κB activity) in conditioned media (CM) generated from microglia under different experimental conditions (control: C-CM; IL-6 stimulated: Stat-CM; IL-6 stimulated in the presence of STAT3 inhibitor: Stat/I$^-$-CM). (a) The levels of phosphorylated (P) forms (active forms) of JNK, STAT3 or NF-κB p65 subunit in astrocyte lysates were evaluated in different experimental groups using PhosphoTracer ELISA kits (Abcam). Incubation of astrocytes with Stat-CM led to significant accumulation of P-JNK or P-STAT3. By contrast, CM from microglia stimulated with IL-6 in the presence of STAT3 inhibitor (Stat/I$^-$-CM) evoked no change in P-JNK or P-STAT3 levels in astrocytes. P-p65 NF-κB levels were also enhanced in astrocytes grown in the presence of Stat-CM. Although not statistically significant, astrocytes challenged with Stat/I$^-$-CM also presented higher levels of P-p65 NF-κB. Fluorescence intensity is expressed as raw fluorescence units (R.F.U.). neg. control: PhosphoTracer ELISA kit negative controls. Each bar is the mean ± SEM of three independent experiments ($n = 3$). $^*p < 0.05$, astrocytes incubated with Stat-CM versus those incubated with C-CM; $^{\#}p < 0.05$, astrocytes incubated with Stat/I$^-$-CM versus cells incubated with Stat-CM. (b) Activation status of NF-κB was further evaluated through immunocytochemistry detection of the p65 NF-κB subcellular distribution. Astrocytes incubated with Stat-CM presented a clear accumulation of p65 NF-κB immunoreactive material (IR) in cell nuclei. In astrocytes incubated with either C-CM or Stat/I$^-$-CM, p65 NF-κB-IR was mainly present in the cytoplasmic compartment and no nuclear transfer of the transcription factor was observed. Pictures are representative of three distinct experiments.

Expression changes in markers of interest

We evaluated the impact of microglial CM on expression of molecules related to astrocytes functions and their reactivity state. In particular, we focused on the levels of mRNAs encoding IL-1β cytokine, growth factors/cytokines (G-CSF, GM-CSF), TLR 2, 3 and 4, Tyrosin receptor kinase B (TrkB) receptor, oxidative stress-associated molecules HO-1 and xCT, gap junction protein connexin 43, GLAST, ATP-sensitive inward rectifying potassium channel KIR4.1 and the astrocyte-specific marker GFAP. Incubation of astrocytes for 6 h with Stat-CM up-regulated mRNA levels of IL-1β CCL2, G-CSF, GM-CSF and TLR2. In the presence of Stat/I$^-$-CM, only limited or no increase in respective mRNA levels were detected. By contrast, the mRNA levels of other examined targets were unaffected after incubation of astrocytes with CM, suggesting that the STAT3 activity-generated microglial CM had a specific and target genes selective modulatory effect (Fig. 4).

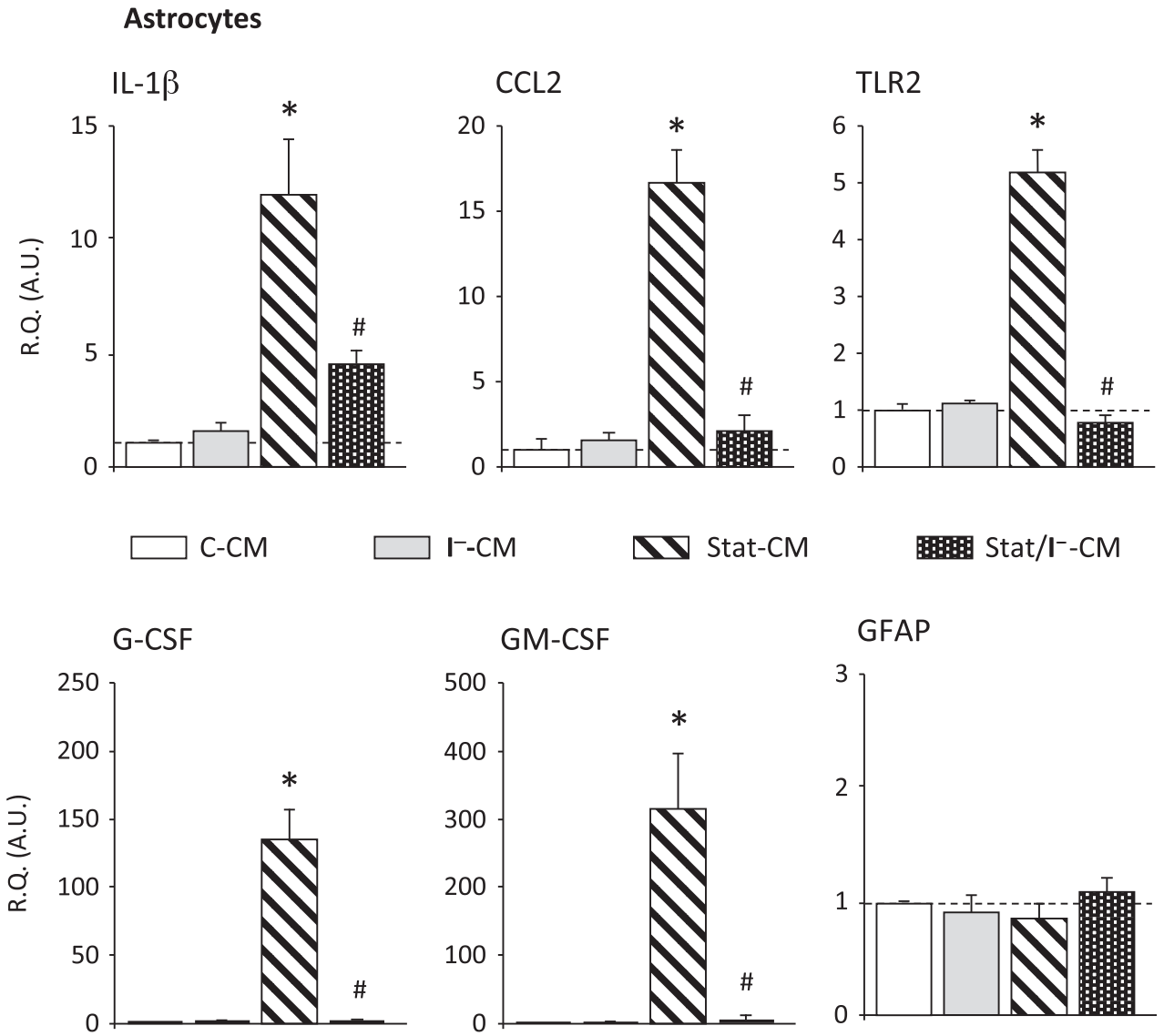

Fig. 4 Janus kinase/signal transduction and activator of transcription 3 (STAT3) activity-generated microglial conditioned media (CM) evoked expression of several markers associated with astrocyte reactivity changes. Incubation of primary astrocytes with CM from microglia with IL-6-activated STAT3 (Stat-CM) for 6 h resulted in an up-regulated expression of mRNA of several markers potentially involved in altered astrocyte signaling [IL-1β, CCL2, granulocyte colony stimulating factor (G-CSF), granulocyte macrophage colony stimulating factor (GM-CSF), toll-like receptor 2, (TLR2)]. These changes were almost completely absent in astrocytes challenged with CM from microglia incubated with IL-6 in the presence of STAT3 inhibitor (Stat/I^{-}CM). C-CM or CM from microglia incubated with STAT3 inhibitor alone (I^{-}-CM) had no impact on the astrocyte expression of evaluated markers. Note that expression of several other markers assessed in this study and related to astrocyte activity, for instance the glial fibrillary acidic protein (GFAP) in this particular case, was not affected after astrocytes incubation with Stat-CM. Each bar is the mean ± SEM (n = 5–6 for each experimental group). *$p < 0.05$, astrocytes incubated with Stat-CM versus those incubated with C-CM; $^{\#}p < 0.05$, astrocytes incubated with Stat/I^{-}-CM versus cells incubated with Stat-CM. In some experiments, relative quantification (R.Q.) corresponding to the ratio of specific mRNA over glyceraldehyde-3-phosphate dehydrogenase mRNA was further evaluated using RS 18S mRNA as reporter gene (A.U.) arbitrary units.

Astrocyte proliferation

Peripheral nerve injury is typically associated with increased glia reactivity and proliferation, and STAT3 signaling was reported to participate in proliferation of astrocytes (Herrmann *et al.* 2008; Tsuda *et al.* 2011). However, *in vitro*, IL-6 is unable to promote astrocytes proliferation on its own (Levinson *et al.* 2000). We confirmed this observation (not shown) and further examined whether microglial STAT3 activation might affect the astrogliosis by detecting and counting cells immunolabeled for the classical cell proliferation marker, KI-67. Total cell number was determined using Hoechst cell nuclei labeling.

Incubation of astrocytes for 24 h with Stat-CM resulted in increased labeling density and higher number of cell nuclei endowed with KI-67-IR as compared with control astrocytes (Fig. 5). In the presence of either I^--CM or Stat/I^--CM, the number of nuclei stained for KI-67-IR was unchanged.

Effect of microglial CM on spinal neurons characteristics

Expression changes of markers of interest

We assessed the effects of the microglial CM on spinal cord neurons by examining the expression changes in a panel of markers expression of which is frequently dysregulated in the spinal cord of animals suffering from neuropathic pain (inflammatory and oxidative stress, neuronal function and excitability). As compared to control cultures, COX-2, iNOS, HO-1 and xCT mRNA levels were significantly enhanced in neurons 6 h after addition of Stat-CM. Incubation of neurons with I^--CM or Stat/I^--CM evoked no significant changes of target mRNAs expression (Fig. 6). The mRNA levels of the other evaluated markers (activating transcription factor 3, MAP2, TrkB receptor, $Na_v1.3$, $Ca_v1.2$) were not affected with any of the microglia-generated CM.

Morphological, connectivity and electrophysiological characteristics

Up-regulated expression of mRNAs encoding markers of inflammatory (COX-2, iNOS) and oxidative stress (HO-1, xCT) conditions suggested a possible deleterious effect of Stat-CM on spinal neurons. In addition to nerve survival, we examined the morphology of nerve processes and the distribution of PSD-95, a marker of glutamatergic synaptic contacts (Peng *et al.* 2013). As compared to control neuron cultures, 24 h incubation of neurons with different CM did not affect the number of NeuN-labeled cells (not shown). However, in the presence of Stat-CM an apparent contraction and thickening of MAP2-stained nerve processes were observed (Fig. 7). Indeed, under such condition, the length of nerve processes was 32.38 ± 6.34% ($p < 0.05$, $n = 15$) less than in cultures incubated with either C-CM, I^--CM or Stat/I^--CM.

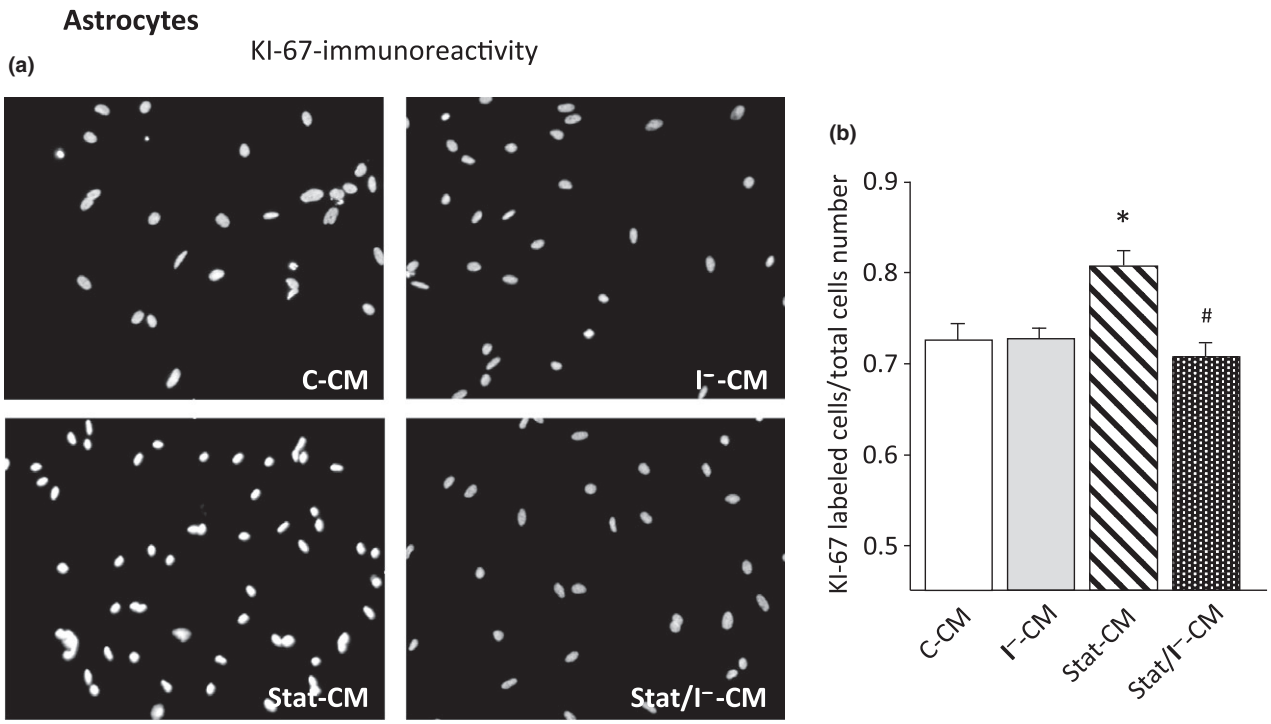

Fig. 5 Proliferation of astrocyte was enhanced following their incubation with microglial CM from microglia with IL-6-activated STAT3 (Stat-CM). (a) Astrocyte cell cultures grown for 24 h in different microglial conditioned media (CM) were stained for KI-67 antigen, a classical marker of cell proliferation. The nuclei were labeled with Hoechst (not shown). (b) For each experimental condition Hoechst-labeled nuclei and those immunostained for KI-67 (both mild and heavy stained) were counted in five randomly selected microscope fields (10× objective). The ratio of KI-67 stained nuclei on the total number of cell nuclei was higher in astrocyte cultures grown in Stat-CM than in those incubated with C-CM, CM from microglia incubated with STAT3 inhibitor alone (I^--CM) or with CM from microglia incubated with IL-6 in the presence of STAT3 inhibitor (Stat/I^-CM). Each bar is the mean ± SEM of three randomly selected fields in 5–6 different experiments ($n = 15$–18). *$p < 0.05$, astrocytes incubated with Stat-CM versus those incubated with C-CM; #$p < 0.05$, astrocytes incubated with Stat/I^--CM versus cells incubated with Stat-CM.

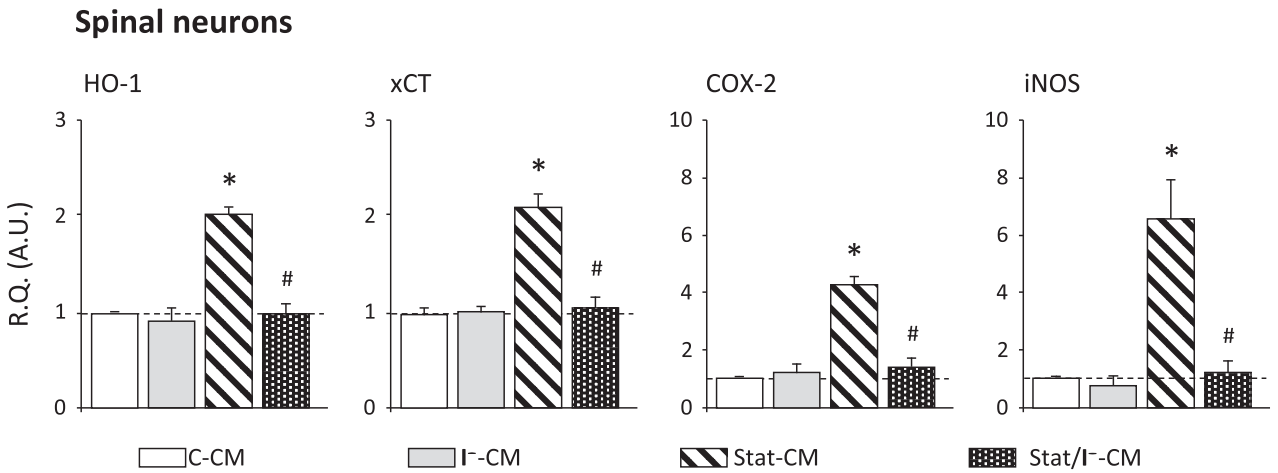

Fig. 6 In spinal cord neurons Janus kinase/signal transduction and activator of transcription 3 (STAT3) activity-generated microglial conditioned media (CM) up-regulated the expression of markers related to inflammatory and oxidative stress. Primary neurons prepared from spinal cord were incubated 6 h with different microglial CM. Between different explored markers, CM from microglia with IL-6-activated STAT3 (Stat-CM) led to a selective increase in mRNA levels of heme oxygenase-1 (HO-1), cystine/glutamate exchanger (xCT), cyclooxygenase-2 (COX-2) and inducible NO synthase (iNOS). Incubation of spinal neurons with other microglial CM evoked no expression change in evaluated mRNAs. The dotted line represents the relative quantification of specific mRNA levels determined in control microglia cultures. Each bar is the mean ± SEM (n = 6–8) for each experimental group). *$p < 0.05$, spinal neurons incubated with Stat-CM versus those incubated with C-CM; #$p < 0.05$, neurons incubated with CM from microglia incubated with IL-6 in the presence of STAT3 inhibitor (Stat/I$^-$CM) versus neurons incubated with Stat-CM. In some experiments relative quantification (R.Q.) corresponding to the ratio of specific mRNA over glyceraldehyde-3-phosphate dehydrogenase mRNA was also evaluated using RS 18S mRNA as reporter gene. A.U., arbitrary units.

Three-dimensional reconstruction showed that the global PSD-95 labeling on neuronal processes was not modified in the presence of Stat-CM. However, the PSD-95-IR dots (in red), regularly distributed along the fine and arborized neurites in control neurons, were mainly localized on the thickened basal part of shortened nerve processes when incubated with Stat-CM (see insets showing accumulating PSD-95-IR spots in neurons cultivated in Stat-CM). This morphological alteration was further documented by changes in the ratio of PSD-95/MAP2-stained volumes, which was significantly lower in spinal neurons grown in Stat-CM than in cultures incubated with C-CM, Stat/I$^-$-CM or I$^-$-CM (Fig. 7). These data suggest that their distribution and density was modified by Stat-CM without changing the global number of PSD-95-stained synaptic contacts.

Under similar experimental condition, we further assessed whether the Stat-CM-evoked morphological changes would be associated with modified neuronal excitability. Using whole-cell patch-clamp configuration, we examined the impact of different CM on cell excitability properties. About 30 neurons from each experimental condition were recorded. During the 15-min recording, we observed no changes in either spontaneous activity or depolarization step-evoked responses in neurons grown in the presence of different CM (not shown). The observed morphological changes and apparent re-arrangement of PSD-95-labeled synaptic contacts had thus no influence on neuron excitability.

Discussion

Using an *in vitro* paradigm based on primary cell cultures, we investigated the influence of microglial JAK/STAT3 activation on neighboring astrocytes and spinal neurons. We mainly focused on the spinal cord markers of biochemical and cell plasticity changes that are frequently associated with neuropathic pain conditions. We showed that activation of this transduction pathway in microglia evoked selective expression of several genes from a panel of 92 explored immune response candidate genes. It also led to substantial changes in the characteristics of microglia-derived culture media that exhibited a modulatory effect on both astrocyte and neuron characteristics. In astrocytes, microglial CM resulting from STAT3 activity (Stat-CM) stimulated several intracellular signaling pathways (JNK, STAT3 and NF-κB) and evoked expression of molecules typically related to astrocyte 'activation'. Stat-CM also promoted the proliferation of astrocytes. In spinal neurons, Stat-CM induced expression of inflammatory and oxidative stress markers. It also affected the morphology of neuronal outgrowths along with the distribution and apparent density of PSD-95 labeling. Although performed in an *in vitro* model, our study supports the idea that, in addition to other signaling events typically observed *in vivo* after peripheral nerve injury, the early activation of JAK/STAT3 pathway in microglia will profoundly impact the signaling from microglia to astrocytes

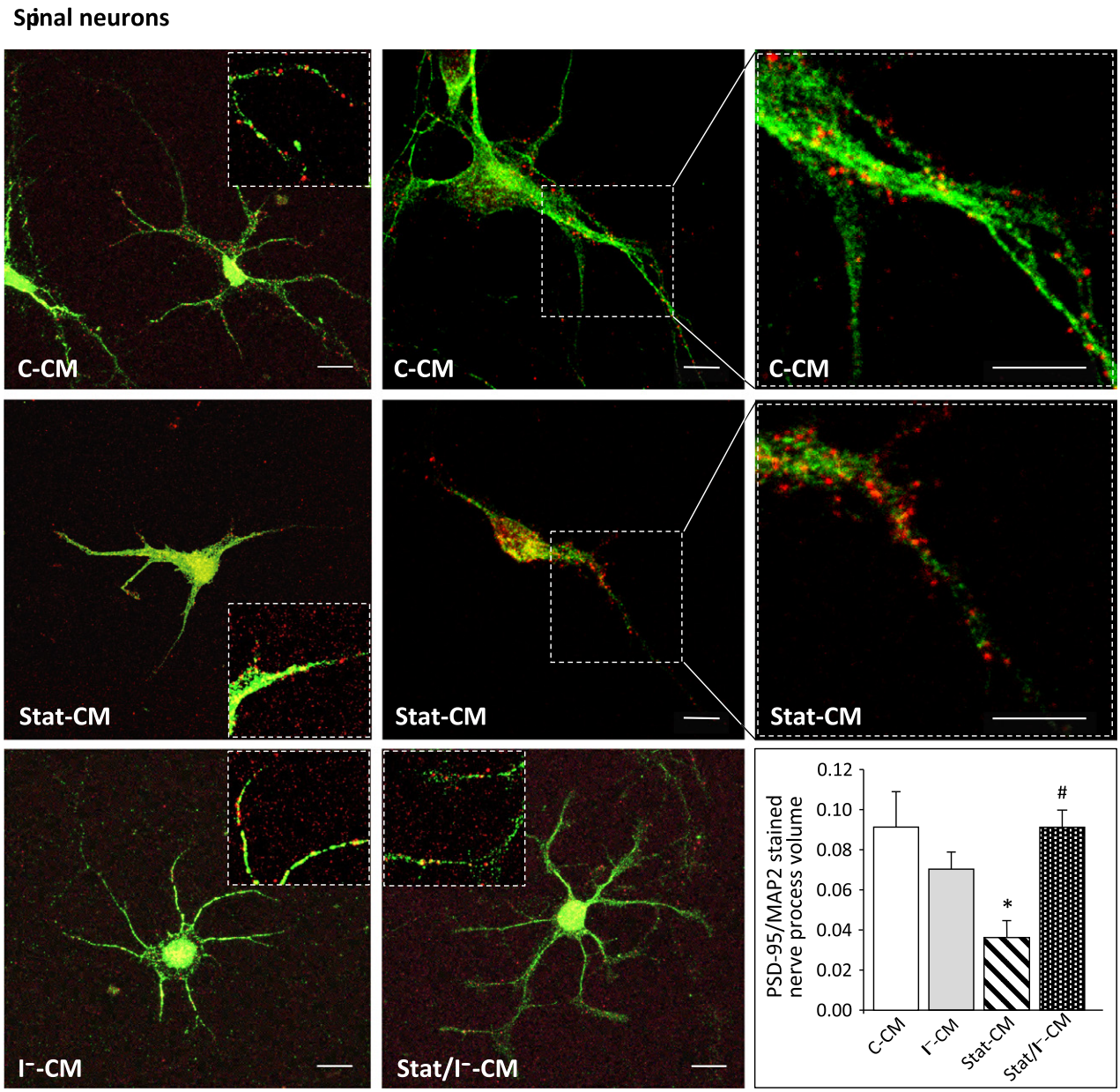

Fig. 7 Microglial conditioned media (CM) altered nerve processes morphology and distribution of the post-synaptic density-95 (PSD-95) protein. Spinal cord primary neurons were challenged with different microglia CM for 24 h then processed for immunofluorescence detection of microtubule-associated protein 2 (MAP2) (in green) and PSD-95 (in red) immunoreactivity. Neurons grown in C-CM presented fine and ramified neurites endowed with PSD-95-labeled dots regularly distributed all along the nerve processes. Incubation of neurons with CM from microglia with IL-6-activated STAT3 (Stat-CM) led to the contraction (neurites length 32.38 ± 6.34% less than in control cultures; $p < 0.05$, $n = 15$) and thickening of nerve process with fewer ramifications. The PSD-95 staining thus appeared more frequently on the thickened bases of neurites, near the cell body (see insets showing details of PSD-95 labeled dots distribution). These alterations were not observed in neurons incubated with CM from microglia incubated with STAT3 inhibitor alone (I^--CM) or CM from microglia incubated with IL-6 in the presence of STAT3 inhibitor (Stat/I^-CM) that showed similar morphology and PSD-95 distribution as controls. Scale bar: 20 μm. Three-dimensional reconstruction of MAP2 and PSD-95 stained volumes (Graph in the Figure, Volocity software; PerkinElmer) showed that though the global PSD-95 staining in neurons grown in Stat-CM remained comparable to that in neurons incubated with C-CM, the ratio of PSD-95/MAP2 labeling was significantly lower. Each bar is the mean ± SEM, *$p < 0.05$ neurons incubated with Stat-CM versus those incubated with C-CM; #$p < 0.05$, neurons incubated with Stat/I^--CM versus Stat-CM, $n = 15$.

and neurons, and thus participate in spinal cord tissue plasticity and remodeling.

We used rat primary cell cultures instead of continuous cell lines, because they may present distinct sensitivity to biological stimuli (M. P., personal observations; Macco *et al.* 2013). A similar pattern of differentially expressed mRNAs was observed in IL-6-stimulated microglia prepared from the rat brain cortex or from the spinal cord. Microglia was, therefore, routinely purified from neonatal rat cortices. As heterogeneous cell cultures containing various cell populations can affect the experimental output, here, particular care was taken to use highly enriched primary cell cultures.

Previous studies based on *in vitro* approaches demonstrated that culture media from activated microglia could modulate the state of astrocytes or neurons. In contrast to our work, these studies mainly used an inflammatory stimulus (lipopolysaccharide, TNFα, interferon gamma etc.) without specifically assessing the consequences of activating a given transduction pathway (see, for instance, Chao *et al.* 1992; Correa *et al.* 2011; Macco *et al.* 2013). Accumulating data indicate a neurotoxic role of activated microglia; though this general conclusion must be carefully examined owing to the particular condition of microglia cultivated *in vitro* (Biber *et al.* 2014).

Intracellular IL-6 signaling is mainly mediated via JAK/STAT3 pathway; though MAPK may also transduce the cytokine signal (Bauer *et al.* 2007). Experiments using the TaqMan® 'mouse immune response' gene expression array showed that expression of some of the targets induced by IL-6 were partially blocked, or even not blocked, by the specific STAT3 inhibitor. This was observed, for instance, with Nfatc – a nuclear factor involved in gene transcription (see Table S1). This observation would suggest that beyond the JAK/STAT3-controlled production of molecules present in CM, other products released from activated microglia could have participated in CM-evoked effects. However, the modulatory effect of Stat-CM on astrocytes and neurons was almost absent using CM generated in the presence of STAT3 inhibitor (Stat/I$^-$CM). This supports the idea that IL-6-activated JAK/STAT3 played a preponderant role in the production of molecules present in CM as well as impacting both astrocyte and neuron characteristics. Additionally, these results also show that no residual IL-6 participated in the reported functional changes.

Exploring the impact of CM on transduction pathways, we observed the presence of phosphorylated p65 NF-κB (using PhopshoTracer system; Abcam) even in astrocytes incubated with Stat/I$^-$CM. However, under these conditions (microglial CM generated in the presence of STAT3 inhibitor) no nuclear translocation of p65 NF-κB subunit was detectable suggesting that NF-κB was mostly transcriptionally inactive.

We did not aim at the characterization of molecules released from microglia after JAK/STAT3 activation and their individual effects. The important spectrum of known target genes of the STAT3 transcription factor and the broad biological effects resulting from STAT3 signaling (Oh *et al.* 2009), together with some molecules identified here and the observed activation of multiple transduction pathways in astrocytes confronted with Stat-CM, suggest a complex impact of microglial STAT3 activity on neighboring cells. For example, the reported IL-18-mediated microglia to astrocyte signaling, leading to NF-κB activation in spinal astrocytes after peripheral nerve injury (Miyoshi *et al.* 2008), probably represents only a part of the multifaceted microglia-astrocyte crosstalk. In addition to NF-κB activation in astrocytes, microglial Stat-CM also evoked the activity of JNK pathway that has been involved in spinal sensitization and neuropathic pain development, in particular through the induction of CCL2 production in spinal astrocytes (Gao *et al.* 2009).

We previously showed that peripheral nerve injury led to a rapid (24 h post-surgery) STAT3 activation mainly in spinal microglia (Dominguez *et al.* 2008). In a similar model of spinal nerve alteration, Tsuda *et al.* (2011) reported delayed (5 days post-injury) STAT3 phosphorylation in astrocytes and implicated STAT3 activity in the spinal astrocyte proliferation that is typically associated with peripheral nerve injury and the emergence of pain. Interestingly, although coming from *in vitro* observations, our data show that microglial STAT3 activity-generated CM contains molecule(s) capable of activating STAT3 in astrocytes and promoting their proliferation. This observation suggests that an initial and rapid post-injury microglia reactivity change involving STAT3 signaling may participate in secondary STAT3 activation in astrocytes that then plays a role in reactive astrogliosis (Okada *et al.* 2006; Herrmann *et al.* 2008; Tsuda *et al.* 2011). This possibility is further supported by data showing that IL-6, unable to evoke astrocyte proliferation on its own, induces expression of molecules that 'secondarily' promote the astrocyte sensitivity to mitogens (Levinson *et al.* 2000).

Astrocytes respond to a large panel of molecules that may engage distinct intracellular pathways and evoke morphological as well as functional changes (Hansen and Malcangio 2013). Despite the activation of these major transduction pathways in the presence of Stat-CM we did not observe any general 'activation' of astrocytes altering the expression of mRNAs encoding several emblematic proteins such as GFAP, GLAST or, for instance, gap junction connexin 43. These data point toward a rather selective regulatory effect of microglial JAK/STAT3 activation and resulting extracellular signaling, though we cannot exclude the possibility that prolonged incubation of cells with Stat-CM (beyond the 6 h exposition used in these experiments) could have up-regulated some additional target mRNA. Indeed, the proliferation of astrocytes evidenced after 24 h incubation in Stat-CM was associated with slight but significant GFAP mRNA level increase (not shown).

Incubation of astrocytes with Stat-CM evoked a marked up-regulation of G-CSF and GM-CSF mRNAs. These cytokines have been recently implicated in both the glia reactivity changes and neuropathic pain. However, experimental data showed these molecules to have a rather complex biological activity profile (depending on the time frame and the route of administration), making it difficult to draw conclusions about their exact role in glia activation, spinal inflammation and pain development (Reddy *et al.* 2009; Liu *et al.* 2011; but see also Chao *et al.* 2012; Guo *et al.* 2013).

In spinal cord neurons, we first assessed the phenotypic changes induced after replacing the culture medium by microglial CM. Similar to what we observed in astrocytes, Stat-CM affected the expression of only certain markers from those assessed. The classical inflammatory condition-associated markers COX-2 and iNOS involved in pain development (Burian and Geisslinger 2005; De Alba *et al.* 2006) were up-regulated. Recently, an elegant study showed that in addition to the immune- and glial cell-mediated prostaglandin production, neuronal COX-2 activity plays a substantial role in inflammatory pain hypersensitivity (Vardeh *et al.* 2011). Our results suggest that activated microglia activity may directly promote spinal neurons COX-2 expression and subsequent prostaglandins production. In the presence of Stat-CM, spinal neurons also contained increased levels of mRNAs, encoding HO-1 and xCT proteins with anti-inflammatory, antioxidant and neuroprotective potency. Classically, the CNS damage-associated induction of these proteins is regulated by Nrf2 transcription factor and localized mainly to non-neuronal cells such as glia, macrophages or meningeal cells (Abbas *et al.* 2011; Wang *et al.* 2014). Activation of these systems in astrocytes is also related to the so-called 'non-cell-autonomous neuroprotection provided in some circumstances by astrocytes (Gupta *et al.* 2012). However, both proteins are also expressed in neurons and participate in antioxidant defense (Lewerenz *et al.* 2012; Chen 2014). Whether the Stat-CM-evoked HO-1 and xCT mRNA expression in spinal neurons involved Nrf2, transcription factor activity remains to be determined. Our data also suggest that astrocytes were less sensitive to the Stat-CM carried oxidative stress signals than primary spinal neurons since no transcriptional changes of HO-1 and xCT mRNA were induced in astrocytes. However, it was also reported that pro-inflammatory activation of astrocytes could mobilize other antioxidant systems not necessarily implicating the Nrf2 target genes (Macco *et al.* 2013).

The multi-task role of microglial in neuronal activity/plasticity control has been increasingly documented. Microglia–neuron interactions play a major role in the developing and damaged CNS, and likely also in the normal healthy CNS (Kettenmann *et al.* 2011). Under various experimental situations, activated microglia CM were shown to affect neuronal survival and neurite outgrowth (Münch *et al.* 2003; Bali *et al.* 2013; for review see Biber *et al.* 2014). It clearly appears that this microglial impact on neuronal networks strongly depends on a specific activating signal that will induce a particular microglial reactive phenotype and certainly also a particular set of released signaling molecules (Li *et al.* 2007; Kettenmann *et al.* 2011). We observed no significant changes in the number of primary spinal neurons after their exposure to Stat-CM for 24 h or even for 48 h. However, in the presence of Stat-CM we consistently observed an apparent thickening and shrinking of nerve processes. We further evaluated the Stat-CM effect on neuronal connectivity, focusing on excitatory NMDA receptors containing synaptic contacts that are preferentially associated with the PSD-95 scaffolding protein. The three dimension microscopic reconstruction of nerve processes showed significant reduction of PSD-95/MAP2 ratio in the presence of Stat-CM. The role of microglia in synaptic contacts remodeling is well documented today. The microglia-mediated 'synaptic stripping' process is mediated through physical microglia–neuron contacts (Kettenmann *et al.* 2011). It has been observed in various pathological conditions, including focal inflammation, and results principally in removal of glutamatergic excitatory synapses (Trapp *et al.* 2007; Kettenmann *et al.* 2011, 2013). Our data suggest that under a particular activation context, products released from microglia may also affect some aspects of spinal neurons connectivity by modulating the morphology of neurites and consequently the distribution of excitatory synaptic contact markers. Using similar experimental protocol, we assessed an eventual impact of these morphological alterations on neuronal excitability. We observed no modification of neuron electrical activities when incubating with Stat-CM. However, further experiments should also evaluate the consequences of a prolonged incubation of neurons with microglia-derived Stat-CM.

Pathological conditions, such as those resulting from peripheral nerve injury, are associated with profound changes in cell environment where numerous signaling molecules released from various cell populations participate in perturbed intercellular signaling. Activation of multiple signal transduction systems, ultimately leading to gene expression changes, plays a major role in tissue remodeling, synaptic plasticity and efficacy. In this complex situation, understanding the exact role of an individual transduction pathway activity is challenging. Despite their limits, *in vitro* approaches may provide an interesting starting point for further *in vivo* studies. In this context, we have shown here that activation of JAK/STAT3 pathway in microglia specifically impacts the characteristics of both astrocytes and spinal neurons. These results support the idea that this pathway activity in microglia has a broad influence on spinal cord tissue under pathological conditions.

Acknowledgments and conflict of interest disclosure

We thank Dr. Nathan Moreau for critical reading of the manuscript. We also thank Bernard Thiev and Jennifer Lavigne for their help with some experiments. JM was recipient of Pfizer post-doc financial support. This work was supported by grants from INSERM, UPMC and Université Paris Descartes. The authors declare no competing interest.

All experiments were conducted in compliance with the ARRIVE guidelines.

Author contributions

JM, AM, MD and MP prepared primary cell cultures. JM and AM performed RT-PCR, WB and ELISA experiments. AM and YB performed immunocytochemistry experiments and DG performed the three dimension reconstruction and microscopic analysis. VA performed electrophysiological recordings. MP, YB and LV conceived and designed the experiments and wrote the manuscript. All authors have read and approved the final version of the manuscript.

Supporting information

Additional supporting information may be found in the online version of this article at the publisher's web-site:

Table S1. Target genes assessed for differential expression and STAT3 inhibition modulatory effect in IL-6 activated microglia.

References

Abbas K., Breton J., Planson A. G., Bouton C., Bignon J., Seguin C., Riquier S., Toledano M. B. and Drapier J. C. (2011) Nitric oxide activates an Nrf2/sulfiredoxin antioxidant pathway in macrophages. *Free Radic. Biol. Med.* **51**, 107–114.

Bali N., Arimoto J. M., Morgan T. E. and Finch C. E. (2013) Progesterone antagonism of neurite outgrowth depends on microglial activation via Pgrmc1/S2R. *Endocrinology* **154**, 2468–2480.

Bareyre F. M., Garzorz N., Lang C., Misgeld T., Büning H. and Kerschensteiner M. (2011) In vivo imaging reveals a phase-specific role of STAT3 during central and peripheral nervous system axon regeneration. *Proc. Natl Acad. Sci. USA* **108**, 6282–6287.

Bauer S., Kerr B. J. and Patterson P. H. (2007) The neuropoietic cytokine family in development, plasticity, disease and injury. *Nat. Rev. Neurosci.* **8**, 221–232.

Biber K., Owens T. and Boddeke E. (2014) What is microglia neurotoxicity (Not)? *Glia* **62**, 841–854.

Burian M. and Geisslinger G. (2005) COX-dependent mechanisms involved in the antinociceptive action of NSAIDs at central and peripheral sites. *Pharmacol. Ther.* **107**, 139–154.

Chao C. C., Hu S., Molitor T. W., Shaskan E. G. and Peterson P. K. (1992) Activated microglia mediate neuronal cell injury via a nitric oxide mechanism. *J. Immunol.* **149**, 2736–2741.

Chao P. K., Lu K. T., Lee Y. L., Chen J. C., Wang H. L., Yang Y. L., Cheng M. Y., Liao M. F. and Ro L. S. (2012) Early systemic granulocyte-colony stimulating factor treatment attenuates neuropathic pain after peripheral nerve injury. *PLoS ONE* **7**, e43680.

Chen J. (2014) Heme oxygenase in neuroprotection: from mechanisms to therapeutic implications. *Rev. Neurosci.* **25**, 269–280.

Correa F., Ljunggren E., Mallard C., Nilsson M., Weber S. G. and Sandberg M. (2011) The Nrf2-inducible antioxidant defense in astrocytes can be both up- and down-regulated by activated microglia: involvement of p38 MAPK. *Glia* **597**, 785–799.

De Alba J., Clayton N. M., Collins S. D., Colthup P., Chessell I. and Knowles R. G. (2006) GW274150, a novel and highly selective inhibitor of the inducible isoform of nitric oxide synthase (iNOS), shows analgesic effects in rat models of inflammatory and neuropathic pain. *Pain* **120**, 170–181.

Dominguez E., Rivat C., Pommier B., Mauborgne A. and Pohl M. (2008) JAK/STAT3 pathway is activated in spinal cord microglia after peripheral nerve injury and contributes to neuropathic pain development in rat. *J. Neurochem.* **107**, 50–60.

Dominguez E., Mauborgne A., Mallet J., Desclaux M. and Pohl M. (2010) SOCS3-mediated blockade of JAK/STAT3 signaling pathway reveals its major contribution to spinal cord neuroinflammation and mechanical allodynia after peripheral nerve injury. *J. Neurosci.* **30**, 5754–5766.

Gao Y. J., Zhang L., Samad O. A., Suter M. R., Yasuhiko K., Xu Z. Z., Park J. Y., Lind A. L., Ma Q. and Ji R. R. (2009) JNK-induced MCP-1 production in spinal cord astrocytes contributes to central sensitization and neuropathic pain. *J. Neurosci.* **29**, 4096–4108.

Goslin K., Asmussen H. and Banker G. (1998) Rat hippocampal neurons in low-density culture, in *Culturing Nerve Cells* (Banker G. and Goslin K., eds), pp. 339–370. MIT press, Cambridge, MA.

Grace P. M., Hutchinson M. R., Maier S. F. and Watkins L. R. (2014) Pathological pain and the neuroimmune interface. *Nat. Rev. Immunol.* **14**, 217–231.

Guo Y., Zhang H., Yang J., Liu S., Bing L., Gao J. and Hao A. (2013) Granulocyte colony-stimulating factor improves alternative activation of microglia under microenvironment of spinal cord injury. *Neuroscience* **238**, 1–10.

Gupta K., Patani R., Baxter P., Serio A., Story D., Tsujita T., Hayes J. D., Pedersen R. A., Hardingham G. E. and Chandran S. (2012) Human embryonic stem cell derived astrocytes mediate non-cell-autonomous neuroprotection through endogenous and drug-induced mechanisms. *Cell Death Differ.* **19**, 779–787.

Hansen R. R. and Malcangio M. (2013) Astrocytes-multitaskers in chronic pain. *Eur. J. Pharmacol.* **716**, 120–128.

Herrmann J. E., Imura T., Song B., Qi J., Ao Y., Nguyen T. K., Korsak R. A., Takeda K., Akira S. and Sofroniew M. V. (2008) STAT3 is a critical regulator of astrogliosis and scar formation after spinal cord injury. *J. Neurosci.* **28**, 7231–7243.

Ji R. R., Berta T. and Nedergaard M. (2013) Glia and pain: is chronic pain a gliopathy? *Pain* **154**(Suppl 1), S10–S28.

Kettenmann H., Hanisch U. K., Noda M. and Verkhratsky A. (2011) Physiology of microglia. *Physiol. Rev.* **91**, 461–553.

Kettenmann H., Kirchhoff F. and Verkhratsky A. (2013) Microglia: new roles for the synaptic stripper. *Neuron* **77**, 10–18.

Kim O. S., Park E. J., Joe E. H. and Jou I. (2002) JAK-STAT signaling mediates gangliosides-induced inflammatory responses in brain microglial cells. *J. Biol. Chem.* **277**, 40594–40601.

Levinson S. W., Jiang F. J., Stoltzfus O. K. and Ducceschi M. H. (2000) IL-6 type cytokines enhances epidermal growth factor-stimulated astrocyte proliferation. *Glia* **32**, 328–337.

Lewerenz J., Maher P. and Methner A. (2012) Regulation of xCT expression and system x (c) (-) function in neuronal cells. *Amino Acids* **42**, 171–179.

Li L., Lu J., Tay S. S., Moochhala S. M. and He B. P. (2007) The function of microglia, either neuroprotection or neurotoxicity, is

determined by the equilibrium among factors released from activated microglia in vitro. *Brain Res.* **1159**, 8–17.

Lim G., Wang S., Zhang Y., Tian Y. and Mao J. (2009) Spinal leptin contributes to the pathogenesis of neuropathic pain in rodents. *J. Clin. Invest.* **119**, 295–304.

Liu J. T., Lui P. W., Liu F. C., Lai Y. S. and Day Y. J. (2011) Exogenous granulocyte colony-stimulating factor exacerbate pain-related behaviors after peripheral nerve injury. *J. Neuroimmunol.* **232**, 83–93.

Livak K. J. and Schmittgen T. D. (2001) Analysis of relative gene expression data using real-time quantitative PCR and the 2(-Delta Delta C(T)) Method. *Methods* **25**, 402–408.

Macco R., Pelizzoni I., Consonni A., Vitali I., Giacalone G., Martinelli Boneschi F., Codazzi F., Grohovaz F. and Zacchetti D. (2013) Astrocytes acquire resistance to iron-dependent oxidative stress upon proinflammatory activation. *J. Neuroinflammation* **10**, 130.

McMahon S. B. and Malcangio M. (2009) Current challenges in glia-pain biology. *Neuron* **15**, 46–54.

Mecha M., Inigo P. M., Mestre L., Hernangomez M., Borell J. and Guaza C. (2011) An easy and fast way to obtain a high number of glial cells from rat cerebral tissue: a beginners approach. *Nat. Protoc. Exch.* doi:10.1038/protex.2011.218.

Meunier A., Latrémolière A., Dominguez E., Mauborgne A., Mallet J., Phillipe S. and Pohl M. (2007) Lentiviral-mediated targeted NF-κB blockade in dorsal spinal cord glia attenuates sciatic nerve injury-induced hyperalgesia in rat. *Mol. Ther.* **15**, 687–697.

Miyoshi K., Obata K., Kondo T., Okamura H. and Noguchi K. (2008) Interleukin-18-mediated microglia/astrocyte interaction in the spinal cord enhances neuropathic pain processing after nerve injury. *J. Neurosci.* **28**, 12775–12787.

Münch G., Gasic-Milenkovic J., Dukic-Stefanovic S., Kuhla B., Heinrich K., Riederer P., Huttunen H. J., Founds H. and Sajithlal G. (2003) Microglial activation induces cell death, inhibits neurite outgrowth and causes neurite retraction of differentiated neuroblastoma cells. *Exp. Brain Res.* **150**, 1–8.

Oh Y. M., Kim J. K., Choi Y., Choi S. and Yoo J. Y. (2009) Prediction and experimental validation of novel STAT3 target genes in human cancer cells. *PLoS ONE* **4**, e6911.

Okada S., Nakamura M., Katoh H. *et al.* (2006) Conditional ablation of Stat3 or Socs3 discloses a dual role for reactive astrocytes after spinal cord injury. *Nat. Med.* **12**, 829–834.

Peng H. Y., Chen G. D., Lai C. Y., Hsieh M. C. and Lin T. B. (2013) Spinal serum-inducible and glucocorticoid-inducible kinase 1 mediates neuropathic pain via kalirin and downstream PSD-95-dependent NR2B phosphorylation in rats. *J. Neurosci.* **33**, 5227–5240.

Reddy P. H., Manczak M., Zhao W., Nakamura K., Bebbington C., Yarranton G. and Mao P. (2009) Granulocyte-macrophage colony-stimulating factor antibody suppresses microglial activity: implication for anti-inflammatory effects in Alzheimer's disease and multiple sclerosis. *J. Neurochem.* **111**, 1514–1528.

Suter M. R., Wen Y. R., Decosterd I. and Ji R. R. (2007) Do glial cells control pain? *Neuron Glia Biol.* **3**, 255–268.

Trapp B. D., Wujek J. R., Criste G. A., Jalabi W., Yin X., Kidd G. J., Stohlman S. and Ransohoff R. (2007) Evidence for synaptic stripping by cortical microglia. *Glia* **55**, 360–368.

Tsuda M., Kohro Y., Yano T. *et al.* (2011) JAK-STAT3 pathway regulates spinal astrocyte proliferation and neuropathic pain maintenance in rats. *Brain* **134**, 1127–1139.

Vardeh D., Wang D., Costigan M., Lazarus M., Saper C. B., Woolf C. J., Fitzgerald G. A. and Samad T. A. (2011) COX2 in CNS neural cells mediates mechanical inflammatory pain hypersensitivity in mice. *J. Clin. Invest.* **119**, 287–294.

Wang X., Campos C. R., Peart J. C., Smith L. K., Boni J. L., Cannon R. E. and Miller D. S. (2014) Nrf2 upregulates ATP binding cassette transporter expression and activity at the blood-brain and blood-spinal cord barriers. *J. Neurosci.* **34**, 8585–8593.

Yin Q., Fan Q., Zhao Y., Cheng M. Y., Liu H., Li J., Lu F. F., Jia J. T., Cheng W. and Yan C. D. (2015) Spinal NF-κB and chemokine ligand 5 expression during spinal glial cell activation in a neuropathic pain model. *PLoS ONE* **10**, e0115120.